Late-stage diversification of indole skeletons through nitrogen atom insertion

Author(s):
Reisenbauer, Julia C.; Green, Ori; Franchino, Allegra; Finkelstein Dobratz, Patrick; Morandi, Bill

Publication date:
2022-09-02

Permanent link:
https://doi.org/10.3929/ethz-b-000568748

Originally published in:
Science 377(6610), https://doi.org/10.1126/science.add1383

Funding acknowledgement:
757608 - Shuttle Catalysis for Reversible Molecular Construction (EC)

Late-stage diversification of indole skeletons through nitrogen atom insertion

Authors: Julia C. Reisenbauer[1§], Ori Green[1§], Allegra Franchino[1], Patrick Finkelstein[1], Bill Morandi[1]*

Affiliations:

[1]Laboratorium für Organische Chemie, ETH Zürich, 8093 Zürich, Switzerland

*Corresponding author. Email: bill.morandi@org.chem.ethz.ch

[§]These authors contributed equally to this work.

Abstract: Compared to peripheral late-stage transformations, mainly focusing on C–H functionalizations, reliable strategies to directly edit the core skeleton of pharmaceutical lead compounds still remain scarce, despite the recent flurry of activity in this area. Herein, we report the skeletal editing of indoles through nitrogen atom insertion, accessing the corresponding quinazoline or quinoxaline bioisosteres via trapping of an electrophilic nitrene species generated from ammonium carbamate and hypervalent iodine. This reactivity relies on the strategic use of a silyl group as a labile protecting group that can suppress the inherent nucleophilicity of the nitrogen in indoles while allowing for subsequent product release. The utility of this highly functional group-compatible methodology in the context of late-stage skeletal editing of several commercial drugs is demonstrated.

One-Sentence Summary: Development of a late-stage indole editing strategy enabled by nitrogen atom insertion to access the bioisosteric quinazolines and quinoxalines.

Main Text:

Major advances in the field of late-stage functionalization have recently unlocked extraordinary structural diversity from common synthetic scaffolds, obviating the resource and time-consuming *de novo* synthesis of a library of derivatives (*1*). The development of numerous, versatile late-stage C–H functionalization strategies to modify target molecules has been a core tenet of this paradigm shift (*2*, *3*), allowing the introduction of key peripheral modifications. In contrast, complementary approaches that can directly modify the underlying core skeleton of a molecule are less common, despite their potential to expand the accessible chemical space (*4–11*). Formal single atom insertion reactions to modify aromatic moieties have proven to be especially challenging given the inherent inertness of aromatic carbon-based skeleton towards cleavage of a carbon-carbon bond (*12*). Despite this formidable challenge, a limited number of carbon (*13–16*) or oxygen (*17*, *18*) insertion or deletion reactions to reshape molecular architectures has been developed. Given the prevalence of nitrogen atoms in biologically active molecules, the direct modification of valuable core structures through single nitrogen atom manipulation is of particular significance (*19*) and especially interesting in the context of evaluating structure-activity relationships in medicinal chemistry settings. Although broad-scope methods to delete a nitrogen atom in molecular scaffolds have been recently disclosed (*20–23*), methods to insert a single nitrogen atom have remained limited, despite their immense potential for the synthesis of ubiquitous *N*-heterocycles. Apart from the classical Beckmann rearrangement of carbonyl derivatives (*24*), these methods are currently either restricted to structural motifs that are not commonly found in nature (e.g. indene, 2-arylindoles) or do not exhibit broad functional group compatibility, preventing their application to late-stage functionalization (*25–32*).

Indoles are among the most widespread nitrogen-containing heterocycles in medicinal chemistry compounds and natural products (*33*) and thus represent an ideal substrate class for the

development of late-stage skeletal editing reactions (*6*). Such an approach is particularly attractive if less naturally abundant, yet pharmaceutically interesting scaffolds, could be rapidly accessed (Fig. 1A). Direct insertion of a nitrogen atom into the indole scaffold would enable straightforward access to *N*,*N*-heterocycles without changing the substitution pattern on the starting indole. This transformation of the indole core into such bioisosteric motifs (*34*, *35*), which are not commonly found as building blocks in medicinal chemistry libraries (*36*) yet are widely recognized as privileged pharmacophores in modern drug discovery (*33*, *37*), could have a transformative impact on the field of late-stage diversification, facilitating the discovery and optimization of drug candidates.

Here we introduce a method for the insertion of a nitrogen atom into indoles affording *N*,*N*-heterocycles. Depending on the substitution pattern of the parent indole structure, either quinazolines or quinoxalines can be selectively accessed. This practical reaction tolerates a broad range of functional groups so that a wide set of natural products and commercial drugs can be transformed into their corresponding bioisosteric analogues.

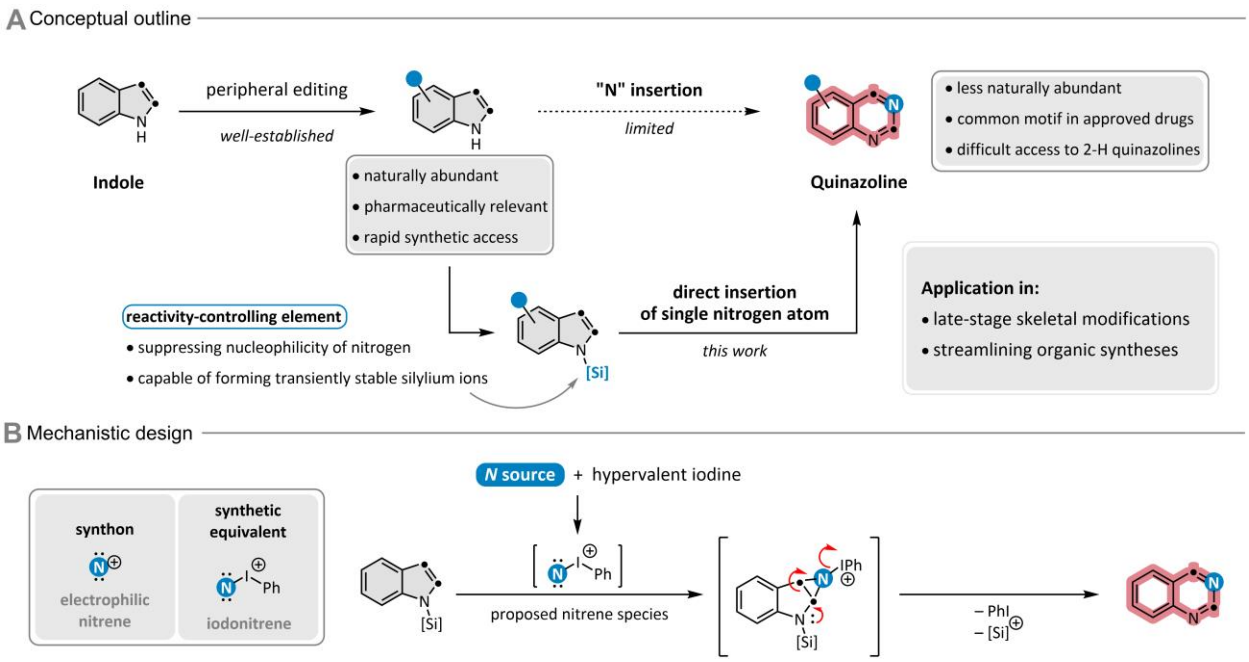

Fig. 1. **Core derivatization of indoles.** (**A**) Diversification of indoles to access pharmaceutically interesting quinazoline motifs. (**B**) Mechanistic design for the transformation of indole skeletons into the corresponding quinazoline scaffold.

To transform indole scaffolds into the corresponding quinazoline motifs, we needed to identify a suitable reagent to act as an electrophilic nitrogen atom donor. We chose to investigate *in-situ* generated electrophilic iodonitrenes, accessed by combining commercially available hypervalent iodine with nitrogen sources (Fig. 1B). In the context of skeletal editing, these reagents have already been harnessed in nitrogen deletion rather than insertion reactions (*22*), besides exhibiting other unique reactivity patterns (*38–40*). In our design, a stepwise (2+1) cycloaddition would initially provide an aziridine intermediate. Subsequent elimination of iodobenzene, followed by aromatization of the reaction intermediate, would facilitate the desired ring expansion reactions towards the quinazoline product (*15*).

A key challenge in the overall design is the inherent nucleophilicity of the unprotected indole nitrogen which could directly react with the electrophilic iodonitrene species. This would lead to the generation of a labile isodiazene intermediate, which would ultimately promote the degradation of the underlying carbon skeleton by the formation of unstable carbon-centered radicals after the release of gaseous nitrogen (Fig. 2A) (*22*). Our design overcomes this intrinsic challenge through the strategic use of a protecting group, which is capable of both suppressing the inherent nucleophilicity of the nitrogen and acting as a sufficiently labile electrofuge to release the product. We investigated silyl-based groups due to their aptitude for stabilizing positively charged intermediates and their potency as electrofuges (*41*). Additionally, the silyl group's susceptibility to hydrolysis can be appropriately adjusted by changing the substituents on the silicon atom (*42*). Indoles bearing silyl-based as well as other commonly used protecting groups, such as *tert*-butyloxycarbonyl (Boc), acetyl (Ac) and methyl, were evaluated under the initial reaction conditions. As might be expected based on the proposed mechanism, only silyl groups were effective in providing the desired quinazoline product **8a** (Fig. 2B), with *tert*-butyldimethyl (TBS) protected indoles undergoing the desired transformation most efficiently.

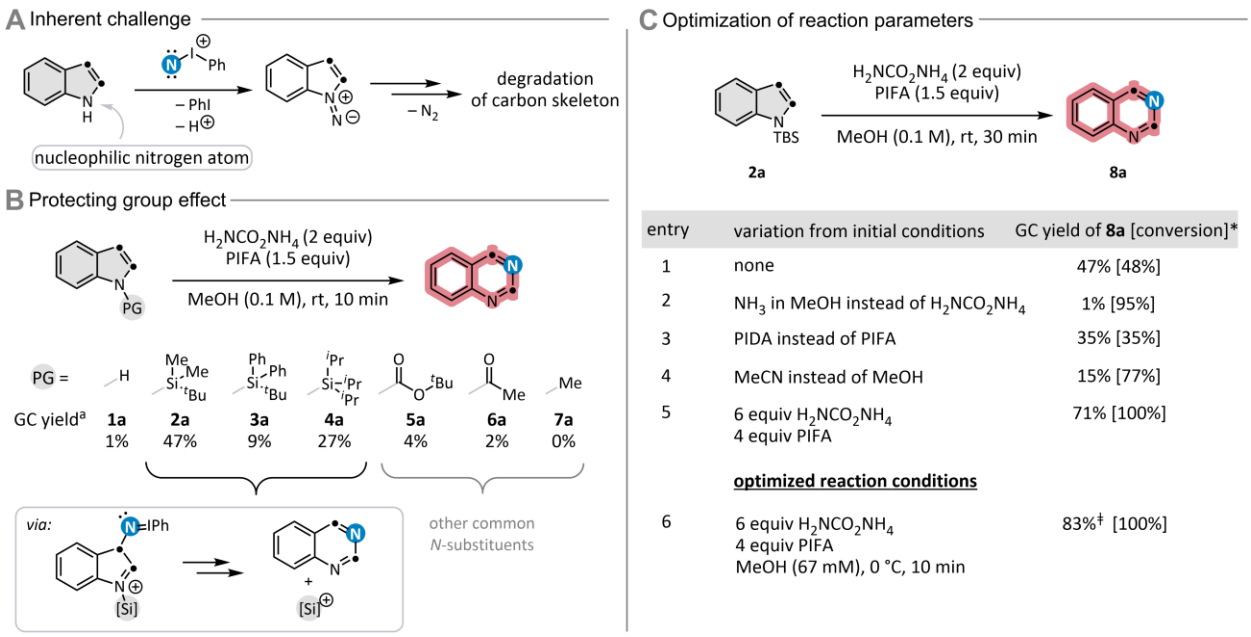

entry	variation from initial conditions	GC yield of **8a** [conversion]*
1	none	47% [48%]
2	NH_3 in MeOH instead of $H_2NCO_2NH_4$	1% [95%]
3	PIDA instead of PIFA	35% [35%]
4	MeCN instead of MeOH	15% [77%]
5	6 equiv $H_2NCO_2NH_4$ 4 equiv PIFA	71% [100%]
	optimized reaction conditions	
6	6 equiv $H_2NCO_2NH_4$ 4 equiv PIFA MeOH (67 mM), 0 °C, 10 min	83%‡ [100%]

Fig. 2. **Reaction development.** (**A**) Inherent challenge associated with the nucleophilicity of the nitrogen in indole substrates. (**B**) Control by labile protecting group to enable product formation. (**C**) Optimization of the nitrogen atom insertion reaction. Reactions were performed on 0.1-mmol scale. *Yield and conversion were determined by GC analysis of the crude reaction mixture using *n*-dodecane as an internal standard. ‡Yield of the isolated product **8a** of a 1.0-mmol scale reaction. PIFA = [bis(trifluoroacetoxy)iodo]benzene, PIDA = (diacetoxyiodo)benzene.

Besides the choice of labile protecting group, the reaction conditions were further optimized by investigating the effect of the other reaction parameters (Fig. 2C). Commercially available [bis-(trifluoroacetoxy)iodo]benzene (PIFA) in methanol in combination with ammonium carbamate as the nitrogen source proved to be the preferred reagent mixture to suppress undesired oxidative decomposition of the indole core and obtain the product in high yield. With the optimized reaction conditions in hand, the scope of the iodonitrene-enabled skeletal ring expansion was explored using this operationally simple protocol (Fig. 3). The compatibility of the nitrogen atom insertion method with diverse substitution patterns as well as common functional groups on the TBS-protected indole precursors was evaluated. Quinazoline products featuring electron-withdrawing

substituents, such as halogens (**8b**–**8f**), esters (**8g**, **8h**), nitriles (**8i**, **8j**), and sulfones (**8k**), as well as electron-donating groups, such as ethers (**8m**–**8o**) and silyl ethers (**8p**), were obtained in moderate to good yields from the corresponding TBS-protected indole precursors. In most cases, except for nitrile-bearing indole precursors, full conversion of the starting materials was observed. Likewise, carboxylic acids (**8l**), alkenes (**8q**) and alkynes (**8r**) were compatible under the optimized reaction conditions. An unprotected piperidine-substituted indole could be transformed into the corresponding product (**8s**), although in lower yield likely due to the propensity of the secondary amine to form isodiazenes leading to degradations. Indole substrates bearing acetals, as well as primary, secondary or tertiary alcohol groups, performed comparably well under the reaction conditions leading to the desired quinazoline products **8t**–**8w**. This strategy also accessed the 1,3,8-triazanaphthaline core (**8x**) from the TBS-protected *aza*-indole in moderate yield (for more details see Supplementary Material). Additionally, indoles bearing adjacent pyridine and benzofuran motifs, common heterocyclic handles, were efficiently transformed into the corresponding quinazoline moieties (**8y**, **8z**). Despite their structural simplicity, synthetic protocols to access most of these quinazolines are unreported, as existing methods do not allow easy access to the 2-H quinazoline products (*43*). TBS-protected indoles featuring substituents on the 2-, 3- or 7-position (**8ab**, **8ac**, **8ad**), as well as 2,3-disubstituted indoles (**8ae**), were successfully converted to the corresponding quinazoline motifs in good yields showing the reaction's compatibility with proximal substituents (Fig. 3B). The identity of product **8ab** was further confirmed by X-ray analysis. This is an important result, as most biologically active indole derivatives are substituted at the 2 and/or 3 position of the indole scaffold (*33*).

Evaluation of a diverse set of indole cores revealed pathways to either quinazoline or quinoxaline scaffolds, depending on the reactant's substituents (Fig. 3C). 2,3-Disubstituted TBS-protected indoles bearing five or six-membered fused rings (**9a**, **9b**) exclusively afforded the corresponding

quinoxaline products (**10a**, **10b**) in good to excellent yields. This result further extends the utility of the protocol since five- and six-membered polycyclic indole scaffolds are prevalent in nature. Thus, straightforward access to less naturally abundant quinoxaline motifs could be streamlined synthetically. To gain deeper insight into the parameters influencing the selectivity, a seven-membered ring fused indole substrate (**9c**) was also tested, which rearranged to the quinazoline-like scaffold. However, due to the inherent ring strain, the reactive intermediate was attacked by the nucleophilic solvent, leading to the corresponding methoxy analogue (**10c**), as confirmed by single-crystal X-ray analysis, preventing rearrangement towards the aromatic quinazoline product. The regioselectivity for the fused five-membered 2,3-disubstituted indole scaffold (**9a**) was further rationalized by DFT calculations, suggesting that a rearrangement to the quinoxaline product is most likely explained by thermodynamic considerations, as the transformation into the corresponding quinazoline would result in the formation of a highly strained, energetically unfavored product (computational details can be found fig. S14) (*44*).

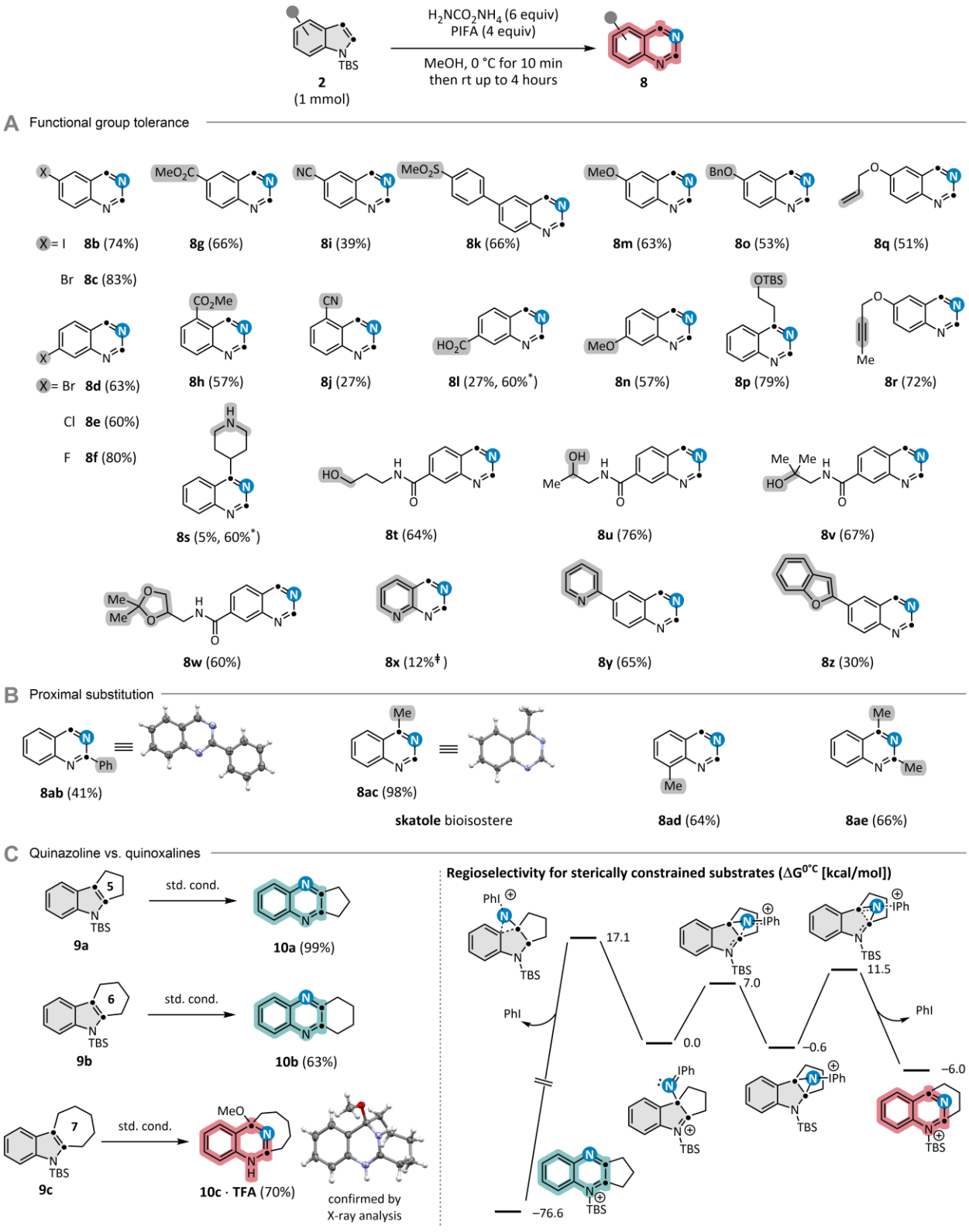

Fig. 3. Substrate scope for the single nitrogen atom insertion. Yields are given for isolated products. Reaction conditions: TBS-indole (1 mmol, 67 mM), ammonium carbamate (6 equiv) and

PIFA (4 equiv) in MeOH at 0 °C for 10 minutes, then at room temperature (rt) for up to 4 hours. (**A**) Investigation of the functional group compatibility of the reaction. (**B**) Effect of proximal substitutions on the reaction outcome. (**C**) Investigating the dependence of the reaction outcome on sterically constrained substrates. DFT calculations for the regioselective preference of substrate **9a**. Gibbs free energies are indicated in kcal/mol at 0 °C. *Yield determined by ^{1}H NMR analysis of the crude reaction mixture using 1,1,2,2-tetrachloroethane or mesitylene as an internal standard. ‡The reaction was performed on 0.2-mmol scale and the product was co-isolated with a side product in an approx. 1:1 ratio (for more details see Supplementary Material).

To illustrate the reaction's potential for expanding accessible chemical space, we applied it to naturally occurring amino acids and commercially available drug molecules (*45*). Protected tryptophan (**11a**) was transformed into the corresponding quinazoline product (**12a**) in good yields. Moreover, the reaction could be performed on 8-mmol scale, demonstrating the scalability of this process. The synthesis of this previously unexplored unnatural amino acid (**12a**) allows for the investigation of its effect on protein and peptide properties (*46*). The skeletal cores of both melatonin (**11b**), a widely encountered neurohormone (*47*), and pindolol (**11c**), a β-adrenoceptor antagonist used for high blood pressure treatments (*48*), were remodeled to afford the corresponding quinazolines **12b** and **12c**, demonstrating the functional compatibility with secondary amines and amides. Similarly, the molecular scaffold of *N*-feruloyl serotonin (**11d**), bearing an α,β-unsaturated amide, was transformed into the quinazoline derivative (**12d**) in excellent yield. Pimprinine-derived substrate (**11e**) as well as analogues of Brevianamide F (**11f**), which both exhibited diverse biological activities, such as fungicidal activities (*49*, *50*), were transformed into the corresponding quinazoline products **12e** and **12f**. Alongside natural products

featuring variable functional handles attached to the core indole scaffold, widely encountered polycyclic indole derivatives have also been shown to possess diverse biological activities and interesting pharmaceutically relevant properties (*51*). Tricyclic tryptoline-3-carboxylic acid (**11g**) was successfully transformed into Lycoperodine-1-derived quinoxaline **12g**. Similarly, 1,2,3,4-tetrahydro-7-methoxycyclopent[*b*]indole-3-acetic acid (**11h**), a key intermediate in the synthesis of APD334, a drug candidate for the treatment of autoimmune diseases (*52*), was transformed into the corresponding quinoxaline core structure **12h**.

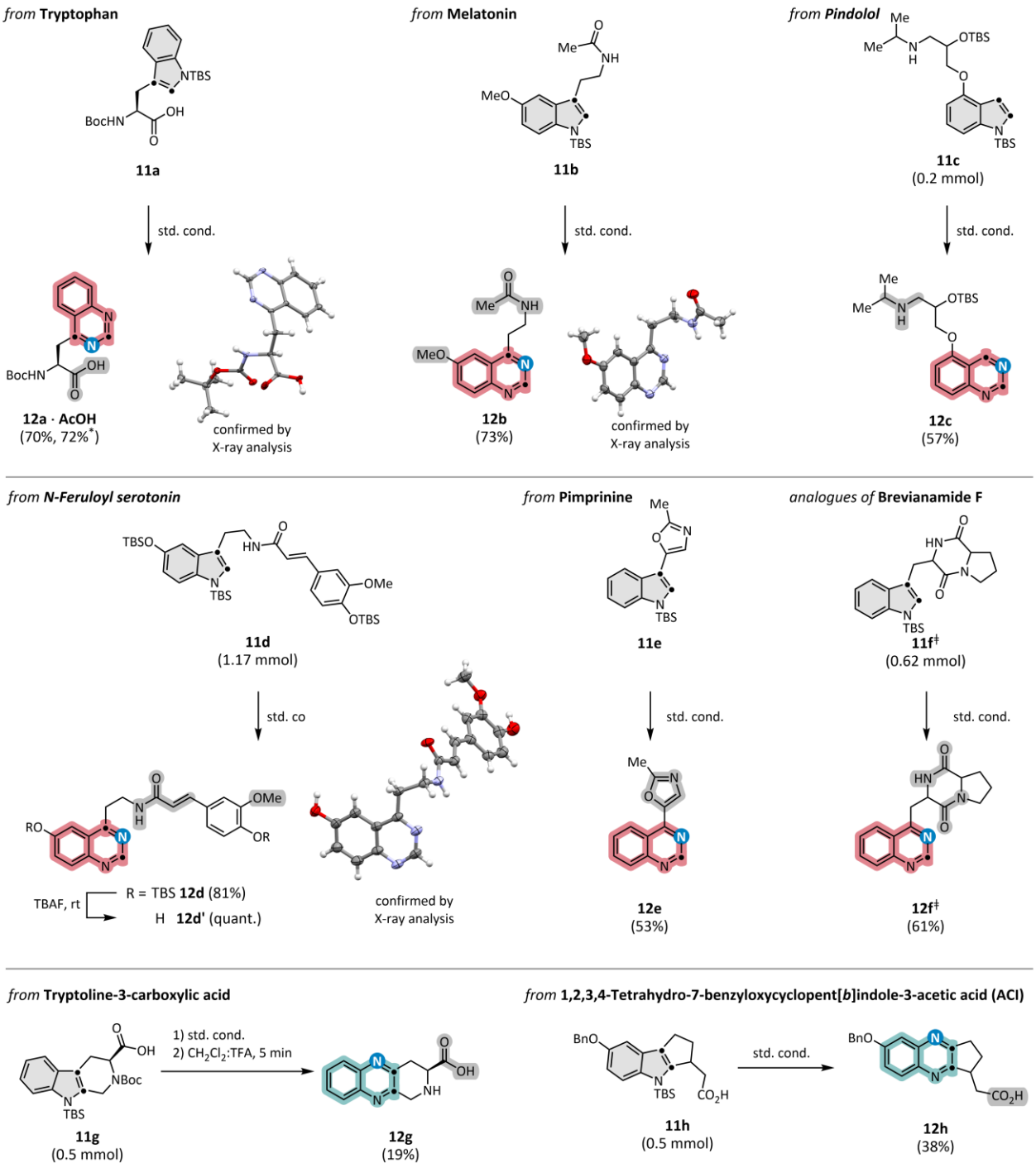

Fig. 4. Late-stage skeletal editing to access quinazoline and quinoxaline scaffolds. Enantiomeric enrichment was not determined. Reactions were performed on 1.0-mmol scale unless otherwise stated. Standard reaction conditions: TBS-indole (1 equiv, 67 mM), $H_2NCO_2NH_4$ (6 equiv) and PIFA (4 equiv) in MeOH at 0 °C for 10 min, then at room temperature for up to 4 hours.

[*]The reaction was performed on 8.0-mmol scale. [‡]Diastereoisomeric ratio 7:3. TBAF = tetra-*n*-butylammonium fluoride, TFA = trifluoroacetic acid.

As indoles are widely encountered, pharmaceutically relevant substrates, we believe that this highly efficient protocol will enable the adoption of more skeletal editing steps in late-stage diversification strategies.

References and Notes

1. D. C. Blakemore, L. Castro, I. Churcher, D. C. Rees, A. W. Thomas, D. M. Wilson, A. Wood, Organic synthesis provides opportunities to transform drug discovery. *Nat. Chem.* **10**, 383–394 (2018).

2. L. Guillemard, N. Kaplaneris, L. Ackermann, M. J. Johansson, Late-stage C–H functionalization offers new opportunities in drug discovery. *Nat. Rev. Chem.* **5**, 522–545 (2021).

3. T. Cernak, K. D. Dykstra, S. Tyagarajan, P. Vachal, S. W. Krska, The medicinal chemist's toolbox for late stage functionalization of drug-like molecules. *Chem. Soc. Rev*. **45**, 546–576 (2016).

4. Y. Hu, D. Stumpfe, J. Bajorath, Recent Advances in Scaffold Hopping. *J. Med. Chem.* **60**, 1238–1246 (2017).

5. H. Lyu, I. Kevlishvili, X. Yu, P. Liu, G. Dong, Boron insertion into alkyl ether bonds via zinc/nickel tandem catalysis. *Science*. **372**, 175–182 (2021).

6. J. Jurczyk, J. Woo, S. F. Kim, B. D. Dherange, R. Sarpong, M. D. Levin, Single-atom logic for heterocycle editing. *Nat. Synth.* **1**, 352–364 (2022).

7. J. B. Roque, Y. Kuroda, L. T. Göttemann, R. Sarpong, Deconstructive diversification of

cyclic amines. *Nature*. **564**, 244–248 (2018).

8. Y. Xia, S. Ochi, G. Dong, Two-Carbon Ring Expansion of 1-Indanones via Insertion of Ethylene into Carbon−Carbon Bonds. *J. Am. Chem. Soc.* **141**, 13038–13042 (2019).

9. Y. Xu, X. Qi, P. Zheng, C. C. Berti, P. Liu, G. Dong, Deacylative transformations of ketones via aromatization-promoted C–C bond activation. *Nature*. **567**, 373–378 (2019).

10. A. J. Smaligo, M. Swain, J. C. Quintana, M. F. Tan, D. A. Kim, O. Kwon, Hydrodealkenylative C(sp^3)–C(sp^2) bond fragmentation. *Science*. **364**, 681–685 (2019).

11. J. Jurczyk, M. C. Lux, D. Adpressa, S. F. Kim, Y.-H. Lam, C. S. Yeung, R. Sarpong, Photomediated ring contraction of saturated heterocycles. *Science*. **373**, 1004–1012 (2021).

12. A. Sattler, G. Parkin, Cleaving carbon–carbon bonds by inserting tungsten into unstrained aromatic rings. *Nature*. **463**, 523–526 (2010).

13. H. Wynberg, E. W. Meijer, in *Organic Reactions* (John Wiley & Sons, Inc., 1982; https://onlinelibrary.wiley.com/doi/10.1002/0471264180.or028.01), pp. 1–36.

14. Z. Wang, L. Jiang, P. S. Sarró, M. G. Suero, Catalytic Cleavage of C(sp^2)−C(sp^2) Bonds with Rh-Carbynoids. *J. Am. Chem. Soc.* **141**, 15509–15514 (2019).

15. B. D. Dherange, P. Q. Kelly, J. P. Liles, M. S. Sigman, M. D. Levin, Carbon Atom Insertion into Pyrroles and Indoles Promoted by Chlorodiazirines. *J. Am. Chem. Soc.* **143**, 11337–11344 (2021).

16. J. Woo, A. H. Christian, S. A. Burgess, Y. Jiang, U. F. Mansoor, M. D. Levin, Scaffold hopping by net photochemical carbon deletion of azaarenes. *Science*. **376**, 527–532 (2022).

17. Z.-C. Cao, Z.-J. Shi, Deoxygenation of Ethers to Form Carbon–Carbon Bonds via Nickel Catalysis. *J. Am. Chem. Soc.* **139**, 6546–6549 (2017).

18. A. Baeyer, V. Villiger, Einwirkung des Caro'schen Reagens auf Ketone. *Chem. Ber.* **32**, 3625–3633 (1899).

19. M. M. Heravi, V. Zadsirjan, Prescribed drugs containing nitrogen heterocycles: an overview. *RSC Adv.* **10**, 44247–44311 (2020).

20. H. Qin, W. Cai, S. Wang, T. Guo, G. Li, H. Lu, N-Atom Deletion in Nitrogen Heterocycles. *Angew. Chem. Int. Ed.* **60**, 20678–20683 (2021).

21. S. H. Kennedy, B. D. Dherange, K. J. Berger, M. D. Levin, Skeletal editing through direct nitrogen deletion of secondary amines. *Nature*. **593**, 223–227 (2021).

22. C. Hui, L. Brieger, C. Strohmann, A. P. Antonchick, Stereoselective Synthesis of Cyclobutanes by Contraction of Pyrrolidines. *J. Am. Chem. Soc.* **143**, 18864–18870 (2021).

23. J. K. Im, I. Jeong, B. Yang, H. Moon, J.-H. Choi, W.-J. Chung, *N*-Chlorinative Ring Contraction of 1,4-Dimethoxyphthalazines via a Bicyclization/Ring-Opening Mechanism. *Synthesis*. **53**, 1760–1770 (2021).

24. E. Beckmann, Zur Kenntniss der Isonitrosoverbindungen. *Chem. Ber.* **19**, 988–993 (1886).

25. S. Liu, X. Cheng, Insertion of ammonia into alkenes to build aromatic N-heterocycles. *Nat. Commun.* **13**, 425 (2022).

26. M. Somei, Y. Kurizuka, A facile route to cinnolines. *Chem. Lett.* **8**, 127–128 (1979).

27. W. E. Noland, D. A. Jones, Novel Ring Expansion and Nitrogen Insertion Reactions of Isatogens. *J. Org. Chem.* **27**, 341–342 (1962).

28. E. J. Moriconi, F. J. Creegan, C. K. Donovan, F. A. Spano, Ring Expansion of 2-Alkyl-1-indanones to Isocarbostyril Derivatives. *J. Org. Chem.* **28**, 2215–2217 (1963).

29. K. Maeda, T. Mishima, T. Hayashi, The Formation of Substituted Quinazolines from Substituted Indoles by the Sensitized Photo-oxygenation in the Presence of Ammonium Acetate. *Bull. Chem. Soc. Jpn.* **47**, 334–338 (1974).

30. Y. Feng, Y. Li, G. Cheng, L. Wang, X. Cui, Copper-Catalyzed Synthesis of 2-Arylquinazolinones from 2-Arylindoles with Amines or Ammoniums. *J. Org. Chem.* **80**, 7099–7107 (2015).

31. M.-M. Xu, W.-B. Cao, X.-P. Xu, S.-J. Ji, Efficient synthesis of 2-arylquinazolin-4-amines via a copper-catalyzed diazidation and ring expansion cascade of 2-arylindoles. *Chem. Commun.* **54**, 12602–12605 (2018).

32. P. R. Kumar, Addition of Phthalimidonitrene to Substituted Indoles. *Heterocycles*. **26**, 1257–1262 (1987).

33. E. Vitaku, D. T. Smith, J. T. Njardarson, Analysis of the Structural Diversity, Substitution Patterns, and Frequency of Nitrogen Heterocycles among U.S. FDA Approved Pharmaceuticals. *J. Med. Chem.* **57**, 10257–10274 (2014).

34. R. A. Smits, I. J. P. de Esch, O. P. Zuiderveld, J. Broeker, K. Sansuk, E. Guaita, G. Coruzzi, M. Adami, E. Haaksma, R. Leurs, Discovery of Quinazolines as Histamine H_4 Receptor Inverse Agonists Using a Scaffold Hopping Approach. *J. Med. Chem.* **51**, 7855–7865 (2008).

35. G. Bouz, S. Bouz, O. Janďourek, K. Konečná, P. Bárta, J. Vinšová, M. Doležal, J. Zitko, Synthesis, Biological Evaluation, and In Silico Modeling of *N*-Substituted Quinoxaline-2-

carboxamides. *Pharmaceuticals*. **14**, 768 (2021).

36. Y. Wang, I. Haight, R. Gupta, A. Vasudevan, What is in Our Kit? An Analysis of Building Blocks Used in Medicinal Chemistry Parallel Libraries. *J. Med. Chem.* **64**, 17115–17122 (2021).

37. V. Alagarsamy, K. Chitra, G. Saravanan, V. R. Solomon, M. T. Sulthana, B. Narendhar, An overview of quinazolines: Pharmacological significance and recent developments. *Eur. J. Med. Chem.* **151**, 628–685 (2018).

38. M. Zenzola, R. Doran, L. Degennaro, R. Luisi, J. A. Bull, Transfer of Electrophilic NH Using Convenient Sources of Ammonia: Direct Synthesis of NH Sulfoximines from Sulfoxides. *Angew. Chem. Int. Ed.* **55**, 7203–7207 (2016).

39. S. Chaabouni, J.-F. Lohier, A. L. Barthelemy, T. Glachet, E. Anselmi, G. Dagousset, P. Diter, B. Pégot, E. Magnier, V. Reboul, One-Pot Synthesis of Aryl- and Alkyl *S*-Perfluoroalkylated *NH*-Sulfoximines from Sulfides. *Chem. Eur. J.* **24**, 17006–17010 (2018).

40. T. Glachet, H. Marzag, N. S. Rosa, J. F. P. Colell, G. Zhang, W. S. Warren, X. Franck, T. Theis, V. Reboul, Iodonitrene in Action: Direct Transformation of Amino Acids into Terminal Diazirines and $^{15}N_2$ -Diazirines and Their Application as Hyperpolarized Markers. *J. Am. Chem. Soc.* **141**, 13689–13696 (2019).

41. H. F. T. Klare, L. Albers, L. Süsse, S. Keess, T. Müller, M. Oestreich, Silylium Ions: From Elusive Reactive Intermediates to Potent Catalysts. *Chem. Rev.* **121**, 5889–5985 (2021).

42. M. Bols, C. M. Pedersen, Silyl-protective groups influencing the reactivity and selectivity

in glycosylations. *Beilstein J. Org. Chem.* **13**, 93–105 (2017).

43. M. Faisal, A. Saeed, Chemical Insights Into the Synthetic Chemistry of Quinazolines: Recent Advances. *Front. Chem.* **8**, 594717 (2021).

44. F. Neese, Software update: The ORCA program system—Version 5.0. *Wiley Interdiscip. Rev. Comput. Mol. Sci. Comput. Mol. Sci.* **12**, e1606 (2022).

45. G. W. Gribble, in *Indole Ring Synthesis: From Natural Products to Drug Discovery* (John Wiley & Sons, Ltd, Chichester, UK, 2016; https://onlinelibrary.wiley.com/doi/full/10.1002/9781118695692.ch1), pp. 1–38.

46. T. Narancic, S. A. Almahboub, K. E. O'Connor, Unnatural amino acids: production and biotechnological potential. *World J. Microbiol. Biotechnol.* **35**, 67 (2019).

47. R. Bolteau, F. Descamps, M. Ettaoussi, D. H. Caignard, P. Delagrange, P. Melnyk, S. Yous, Quinazoline and phthalazine derivatives as novel melatonin receptor ligands analogues of agomelatine. *Eur. J. Med. Chem.* **189**, 112078 (2020).

48. W. H. Aellig, Pindolol-A-b-Adrenoceptor Blocking Drug with Partial Agonist Activity: Clinical Pharmacological Considerations. *Br. J. Clin. Pharmac.* **13**, 187–192 (1982).

49. B. Liu, R. Li, Y. Li, S. Li, J. Yu, B. Zhao, A. Liao, Y. Wang, Z. Wang, A. Lu, Y. Liu, Q. Wang, Discovery of Pimprinine Alkaloids as Novel Agents against a Plant Virus. *J. Agric. Food Chem.* **67**, 1795–1806 (2019).

50. S. Nishanth Kumar, V. Sukumari Nath, R. Pratap Chandran, B. Nambisan, Cyclic dipeptides from rhabditid entomopathogenic nematode-associated Bacillus *cereus* have antimicrobial activities. *World J Microbiol Biotechnol*. **30**, 439–449 (2014).

51. W. Chen, Y. Ma, W. He, Y. Wu, Y. Huang, Y. Zhang, H. Tian, K. Wei, X. Yang, H.

Zhang, Structure units oriented approach towards collective synthesis of sarpagine-ajmaline-koumine type alkaloids. *Nat. Commun.* **13**, 908 (2022).

52. A. Garrido Montalban, Y.-A. Ma, S. Johannsen, S. Tandel, M. J. Martinelli, A novel Fischer pseudo-benzylic decarboxylation approach to the 1,2,3,4-tetrahydro-cyclopenta[*b*]indol-3-yl system. *Tetrahedron Lett.* **56**, 378–381 (2015).

53. CrysAlisPro and AB SPACK. Rigaku Oxford Diffraction (2016).

54. G. M. Sheldrick, SHELXT – Integrated space-group and crystal-structure determination. *Acta Cryst*. **A71**, 3–8 (2015).

55. G. M. Sheldrick, A short history of SHELX. *Acta Cryst*. **A64**, 112–122 (2008).

56. G. M. Sheldrick, Crystal structure refinement with SHELXL. *Acta Cryst*. **C71**, 3–8 (2015).

57. O. V. Dolomanov, L. J. Bourhis, R. J. Gildea, J. A. K. Howard, H. Puschmann, OLEX2: a complete structure solution, refinement and analysis program. *J. Appl. Cryst*. **42**, 339–341 (2009).

58. V. Pirenne, E. G. L. Robert, J. Waser, Catalytic (3 + 2) annulation of donor–acceptor aminocyclopropane monoesters and indoles. *Chem. Sci*. **12**, 8706–8712 (2021).

59. I. Medina-Mercado, E. O. Asomoza-Solís, E. Martínez-González, V. M. Ugalde-Saldívar, L. G. Ledesma-Olvera, J. E. Barquera-Lozada, V. Gómez-Vidales, J. Barroso-Flores, B. A. Frontana-Uribe, S. Porcel, Ascorbic Acid as an Aryl Radical Inducer in the Gold-Mediated Arylation of Indoles with Aryldiazonium Chlorides. *Chem. – A Eur. J.* **26**, 634–642 (2020).

60. X. C. Cambeiro, N. Ahlsten, I. Larrosa, Au-Catalyzed Cross-Coupling of Arenes via Double C-H Activation. *J. Am. Chem. Soc*. **137**, 15636–15639 (2015).

61. S. Minakata, H. Miwa, K. Yamamoto, A. Hirayama, S. Okumura, Diastereodivergent Intermolecular 1,2-Diamination of Unactivated Alkenes Enabled by Iodine Catalysis. *J. Am. Chem. Soc*. **143**, 4112–4118 (2021).

62. Y. Koizumi, H. Kobayashi, T. Wakimoto, T. Furuta, T. Fukuyama, T. Kan, Total synthesis of (-)-serotobenine. *J. Am. Chem. Soc*. **130**, 16854–16855 (2008).

63. Y. Y. Peng, J. Liu, X. Lei, Z. Yin, Room-temperature highly efficient Suzuki–Miyaura reactions in water in the presence of Stilbazo. *Green Chem.* **12**, 1072–1075 (2010).

64. N. A. Isley, F. Gallou, B. H. Lipshutz, Transforming Suzuki-Miyaura cross-couplings of MIDA boronates into a green technology: No organic solvents. *J. Am. Chem. Soc*. **135**, 17707–17710 (2013).

65. D. Perrotta, M.-M. Wang, J. Waser, Lewis Acid Catalyzed Enantioselective Desymmetrization of Donor-Acceptor meso -Diaminocyclopropanes. *Angew. Chemie Int. Ed*. **57**, 5120–5123 (2018).

66. N. Hussain, G. Frensch, J. Zhang, P. J. Walsh, Chemo- and Regioselective C(sp^3)–H Arylation of Unactivated Allylarenes by Deprotonative Cross-Coupling. *Angew. Chemie Int. Ed*. **53**, 3693–3697 (2014).

67. M. Amat, F. Seffar, N. Llor, J. Bosch, Preparation and Reactions of 4-, 5-, and 6-Methoxy Substituted 3-Lithioindoles and 3-Indolylzinc Derivatives. *Synthesis*. **2001**, 267–275 (2001).

68. M. Yokoyama, M. Nomura, H. Togo, H. Seki, Coupling of ribofuranosyl fluoride and indoles. *J. Chem. Soc. Perkin Trans*. **1**, 2145–2149 (1996).

69. X. H. Xu, G. K. Liu, A. Azuma, E. Tokunaga, N. Shibata, Synthesis of indole and biindolyl triflones: Trifluoromethanesulfonylation of indoles with Tf_2O/TTBP (2,4,6-tri- tert -butylpyridine) system. *Org. Lett*. **13**, 4854–4857 (2011).

70. S. Islam, I. Larrosa, On water phosphine-free palladium-catalyzed room temperature C–H arylation of indoles. *Chem. Eur. J.* **19**, 15093–15096 (2013).

71. D. Dhanak, C. B. Reese, Studies in the protection of pyrrole and indole derivatives. *J. Chem. Soc. Perkin Trans*. **1**, 2181–2186 (1986).

72. S. M. Wales, M. M. Walker, J. S. Johnson, Asymmetric synthesis of indole homo-Michael adducts via dynamic kinetic Friedel-Crafts alkylation with cyclopropanes. *Org. Lett*. **15**, 2558–2561 (2013).

73. P. A. Grieco, Y. S. Hon, A. Perez-Medrano, Convergent, enantiospecific total synthesis of the novel cyclodepsipeptide (+)-jasplakinolide (jaspamide). *J. Am. Chem. Soc*. **110**, 1630–1631 (1988).

74. J. Xiang, J. Wang, M. Wang, X. Meng, A. Wu, One-pot total synthesis: The first total synthesis of chiral alkaloid pimprinol A and the facile construction of its natural congeners from amino acids. *Tetrahedron*. **70**, 7470–7475 (2014).

75. A. Garrido Montalban, Y.-A. Ma, S. Johannsen, S. Tandel, M. J. Martinelli, A novel Fischer pseudo-benzylic decarboxylation approach to the 1,2,3,4-tetrahydro-cyclopenta[b]indol-3-yl system. *Tetrahedron Lett*. **56**, 378–381 (2015).

76. S. Sharma, D. Bhattacherjee, P. Das, Oxalic/ Malonic Acids as Carbon Building Block for Benzazoles, Quinazoline and Quinazolinones Synthesis. *Org. Biomol. Chem*. **16**, 1337–1342 (2018).

77. A. Chilin, G. Marzaro, S. Zanatta, V. Barbieri, G. Pastorini, P. Manzini, A. Guiotto, A new access to quinazolines from simple anilines. *Tetrahedron*. **62**, 12351–12356 (2006).

78. C. Xu, F. C. Jia, Z. W. Zhou, S. J. Zheng, H. Li, A. X. Wu, Copper-Catalyzed Multicomponent Domino Reaction of 2-Bromoaldehydes, Benzylamines, and Sodium Azide for the Assembly of Quinazoline Derivatives. *J. Org. Chem*. **81**, 3000–3006 (2016).

79. C. Y. Chen, F. He, G. Tang, H. Yuan, N. Li, J. Wang, R. Faessler, Synthesis of Quinazolines via an Iron-Catalyzed Oxidative Amination of N-H Ketimines. *J. Org. Chem*. **83**, 2395–2401 (2018).

80. D. Zhao, M. X. Zhu, Y. Wang, Q. Shen, J. X. Li, Pd(0)-catalyzed benzylic arylation–oxidation of 4-methylquinazolines via sp3 C–H activation under air conditions. *Org. Biomol. Chem*. **11**, 6246–6249 (2013).

81. M. Y. Chang, T. W. Lee, R. T. Hsu, T. L. Yen, Synthesis of quinoxaline analogues. *Synthesis*. **2011**, 3143–3151 (2011).

82. T. B. Nguyen, P. Retailleau, Elemental Sulfur as Reaction Medium for the Synthesis of Fused Nitrogen Heterocycles by Oxidative Coupling between Cycloalkanones and Nitrogen Nucleophiles. *Adv. Synth. Catal*. **359**, 3843–3847 (2017).

83. H. Kessler, Detection of Hindered Rotation and Inversion by NMR Spectroscopy. *Angew. Chemie Int. Ed*. **9**, 219–235 (1970).

84. C. Bannwarth, S. Ehlert, S. Grimme, GFN2-xTB - An Accurate and Broadly Parametrized Self-Consistent Tight-Binding Quantum Chemical Method with Multipole Electrostatics and Density-Dependent Dispersion Contributions. *J. Chem. Theory Comput*. **15**, 1652–1671 (2019).

85. C. Bannwarth, E. Caldeweyher, S. Ehlert, A. Hansen, P. Pracht, J. Seibert, S. Spicher, S. Grimme, Extended tight-binding quantum chemistry methods. *Wiley Interdiscip. Rev. Comput. Mol. Sci*. **11**, e1493 (2021).

86. S. Grimme, Exploration of Chemical Compound, Conformer, and Reaction Space with Meta-Dynamics Simulations Based on Tight-Binding Quantum Chemical Calculations. *J. Chem. Theory Comput*. **15**, 7169–7192 (2019).

87. P. Pracht, F. Bohle, S. Grimme, Automated exploration of the low-energy chemical space with fast quantum chemical methods. *Phys. Chem. Chem. Phys*. **22**, 7169–7192 (2020).

88. S. Grimme, F. Bohle, A. Hansen, P. Pracht, S. Spicher, M. Stahn, Efficient Quantum Chemical Calculation of Structure Ensembles and Free Energies for Nonrigid Molecules. *J. Phys. Chem. A*. **125**, 4039–4054 (2021).

89. F. Neese, Software update: The ORCA program system—Version 5.0. *Wiley Interdiscip. Rev. Comput. Mol. Sci*. **12**, e1606 (2022).

90. A. D. Becke, Density-functional exchange-energy approximation with correct asymptotic behavior. *Phys. Rev. A*. **38**, 3098–3100 (1988).

91. J. P. Perdew, Density-functional approximation for the correlation energy of the inhomogeneous electron gas. *Phys. Rev. B*. **33**, 8822–8824 (1986).

92. F. Weigend, R. Ahlrichs, Balanced basis sets of split valence, triple zeta valence and quadruple zeta valence quality for H to Rn: Design and assessment of accuracy. *Phys. Chem. Chem. Phys*. **7**, 3297–3305 (2005).

93. S. Grimme, S. Ehrlich, L. Goerigk, Effect of the damping function in dispersion corrected density functional theory. *J. Comput. Chem*. **32**, 1456–1465 (2011).

94. S. Grimme, J. Antony, S. Ehrlich, H. Krieg, A consistent and accurate ab initio parametrization of density functional dispersion correction (DFT-D) for the 94 elements H-Pu. *J. Chem. Phys*. **132**, 154104 (2010).

95. F. Weigend, Accurate Coulomb-fitting basis sets for H to Rn. *Phys. Chem. Chem. Phys*. **8**, 1057–1065 (2006).

96. V. Barone, M. Cossi, Quantum calculation of molecular energies and energy gradients in solution by a conductor solvent model. *J. Phys. Chem. A.* **102**, 1995–2001 (1998).

97. C. Brunken, K.-S. Csizi, S. A. Grimmel, S. Gugler, J.-G. Sobez, M. Steiner, P. L. Türtscher, J. P. Unsleber, A. C. Vaucher, T. Weymuth, M. Reiher, Qcscine/Readuct: Release 3.0.0. Zenodo (2021), doi:10.5281/ZENODO.5782849.

98. Y. Zhao, D. G. Truhlar, Design of density functionals that are broadly accurate for thermochemistry, thermochemical kinetics, and nonbonded interactions. *J. Phys. Chem. A.* **109**, 5656–5667 (2005).

99. A. V. Marenich, C. J. Cramer, D. G. Truhlar, Universal solvation model based on solute electron density and on a continuum model of the solvent defined by the bulk dielectric constant and atomic surface tensions. *J. Phys. Chem. B.* **113**, 6378–6396 (2009).

100. Chemcraft - Citation, (available at https://www.chemcraftprog.com/citation.html).

101. A. Tota, M. Colella, C. Carlucci, A. Aramini, G. Clarkson, L. Degennaro, J. A. Bull, R. Luisi, N−N Bond Formation Using an Iodonitrene as an Umpolung of Ammonia: Straightforward and Chemoselective Synthesis of Hydrazinium Salts. *Adv. Synth. Catal*. **363**, 194–199 (2021).

102. M. Zenzola, R. Doran, L. Degennaro, R. Luisi, J. A. Bull, Transfer of Electrophilic NH Using Convenient Sources of Ammonia: Direct Synthesis of NH Sulfoximines from Sulfoxides. *Angew. Chem. Int. Ed*. **55**, 7203–7207 (2016).

103. J. F. Lohier, T. Glachet, H. Marzag, A. C. Gaumont, V. Reboul, Mechanistic investigation of the NH-sulfoximination of sulfide. Evidence for λ^6-sulfanenitrile intermediates. *Chem. Commun*. **53**, 2064–2067 (2017).

Acknowledgments:

The authors thank the NMR and X-ray service (SMoCC), as well as the Molecular and Biomolecular Analysis Service (MoBiAS) of ETH Zürich for technical assistance. The authors also thank the Morandi group for critical proofreading.

Funding: This project received funding from the European Research Council under the European Union's Horizon 2020 research and innovation program (Shuttle Cat, Project ID: 757608) and was also financially supported by ETH Zürich. JCR acknowledges a fellowship of the Stipendienfonds der Schweizerischen Chemischen Industrie (SSCI). OG acknowledges a fellowship of the International Human Frontier Science Program Organization (LT000861/ 2020-L).

Author contributions: JCR conceived the project. JCR, OG and AF performed the experiments. PF performed the DFT studies. BM supervised the research. JCR, OG and BM wrote the MS. All authors revised and approved the MS.

Competing interests: The authors declare no competing interests.

Data and materials availability: X-ray data for compounds (**8n'**, **8ab**, **8ac**, **10c**, **12a**, **12b, 12d'**) are freely available at the Cambridge Crystallographic Data Centre under deposition numbers 2173003, 2173004, 2171863, 2171881, 2171882, 2172251, 2174296.

Supplementary Materials

Materials and Methods

Supplementary Text

Figs. S1 to S23

Tables S1 to S15

xyz file with Cartesian coordinates